

# Revealing the Intrinsic Magnetism of Non-Magnetic Glasses

Giancarlo Jug<sup>a,b,c</sup> and Sandro Recchia<sup>a</sup>

<sup>a</sup>Dipartimento di Scienza ed Alta Tecnologia  
Università dell'Insubria, Via Valleggio 11, 22100 Como (Italy)

<sup>b</sup>INFN – Sezione di Pavia, Italy

<sup>c</sup>To.Sca.Lab, Dipartimento di Scienza ed Alta Tecnologia, Università dell'Insubria

November 2, 2021

## Abstract

Ordinary multi-component silicate glasses belong to a class of amorphous insulators normally displaying no special form of magnetism, save for the Larmor dominant diamagnetism from the constituent atoms' core electrons and the extrinsic Langevin paramagnetism due to the ubiquitous Fe-group dilute paramagnetic impurities. Here we show that the macroscopic magnetisation of three case-study glass types measured in a SQUID-magnetometer cannot be explained solely by means of the Larmor-Langevin contributions. In particular, we reveal a novel *intrinsic* contribution to the bulk magnetisation due to the amorphous structure itself, a contribution that is peculiar both in its temperature and magnetic-field dependence and represents the first true magnetic effect in nominally non-magnetic glasses. The only theoretical interpretation we know of for such an effect and which can consistently explain the experimental data demands the re-thinking of the atomic organisation of glasses at the nanometric scale.

**A. Introduction.** Glasses are ubiquitous substances known to mankind since pre-history and yet still presenting many unsolved mysteries to the inquisitive scientific mind. What is the precise nature of the atomic structure of glasses, especially at medium-range (MR) scales and determining the physical properties of these non-crystalline solids? Are glasses just dynamically arrested liquids or rather a peculiar new type of solids? What degrees of freedom truly control the onset of vitrification, i.e. the glass “transition”, and conversely: how best to describe the melting of a glass? How can we describe theoretically their physical properties on the basis of a universal, composition-independent modeling framework that would allow for the theoretical control and engineering of the desired glass properties? All of these questions and the quest for new technically exploitable or interesting physical effects make glasses a very much active and attractive field of research in condensed matter physics.

Where the first of the above questions is concerned – MR structure – several scenarios have been proposed over the last hundred years [1, 2, 3, 4, 5, 6, 7, 8, 9, 10, 11]. A much acclaimed approach considers (so-called) network glasses as continuously- and homogeneously-disordered media at the local (atomic), MR and long-range length scale: it is the so-called continuous-random-network (CRN) model of Zachariasen and Warren [3, 4]. However, other scientists have suggested to further elaborate upon the CRN approach in favour of heterogeneous mesoscopic scenarios [1, 2, 5, 6, 7, 10]. Moreover, scenarios have been proposed where the dynamical heterogeneities (DH) known to characterise the supercooled liquid state [13] continue to exist (albeit somewhat more statically) also below  $T_g$ , the nominal temperature of glass formation [8, 9, 11, 12]. One of these non-CRN scenarios views glasses as made up of solid-like particle regions jammed together somewhat below  $T_g$  and presenting liquid-like regions in-between [11]. Remarkably, the liquid-like regions between the solid ones may become the sources of collective orbital magnetic moments that appear to generate an *intrinsic* contribution to the glass sample’s magnetisation mimicking the known Langevin paramagnetism from isolated impurities. In the ordinary silicate glasses the latter are typically from Fe and the Fe-group trace elements [14]. The extra intrinsic magnetic moments issue from specialized, magnetic-field sensitive tunneling systems (TS) believed to be responsible for a plethora of magnetic effects at low temperatures in glasses [11, 15, 16]. These and the more standard TS (the so-called two-level systems (TLS) [17, 18, 16]) might be part of the degrees of freedom sought for in order to investigate the physical properties of glasses at higher temperatures too [19].

In current strategic terms, as it turns out, a better characterisation of the standard TLS (which are parasitic yet ubiquitous defects in glasses) is paramount for high-technology developments and crucial to awaited breakthroughs. For example in fields like the improved detection of gravitational waves [20, 21], the fabrication of coherent qubits for superconductor-based quantum computers [22], and noise-reduction within quantum-information repeaters (quantum memories) in fiber-glass optical transmission [23, 24, 25]. A better understanding of the atomic nature of the TS is therefore also long awaited for [16].

In this Letter we present what we believe to be an important contribution to furthering knowledge in all of the above-mentioned basic and advanced research areas by providing the first report of the exotic and genuinely-magnetic effect in glasses consistent with the theory briefly outlined above [11, 14, 15]. A completely new physical effect in glasses, which is weak but laden with important consequences.

We have investigated experimentally and theoretically three case-study systems within the class of multi-component silicate glasses: Edmund Optics’ BK7 (boro-silicate best optical glass, with main composition  $K_2O-B_2O_3-Na_2O-SiO_2$ ); Schott’s Duran (boro-silicate best chemistry glass, main composition  $Al_2O_3-Na_2O-B_2O_3-SiO_2$ ) and Heraeus’ IP-211-clear (bario-allumino-silicate coating glass, main composition  $CaO-Al_2O_3-BaO-SiO_2$ , hereafter termed BAS in short). However, we have good reasons to believe that our findings and their possible explanation (with appropriate revealing conditions and different main microscopic players) should be pertinent to all amorphous solids (bulk glasses and amorphous films, though not necessarily to the non-atomistic colloidal glasses).

We have systematically investigated the dependence of  $M$  (the macroscopic magnetisation of point-like samples) on  $T$  (temperature) and  $H$  (magnetic field), in the range  $2 \leq T \leq 315$  K and  $0.5 \leq H \leq 65$  kOe by means of a SQUID-magnetometer and for the above-mentioned glassy solids. In such insulating glasses, the SQUID-characterisation is normally employed to assess the trace-like (ppm) content of paramagnetic impurities (iron, typically) from a single  $M$  vs.  $1/T$  chart at fixed  $H$ . The idea, never challenged thus far (however, see [14]), has been that only  $Fe^{3+}$  is present in such systems. Then, the best-fit to the data with the textbook form [26] (hereafter already extended for more than one paramagnetic species):

$$M(T, H) = -\chi_L H + \sum_{s=Fe^{2+}, Fe^{3+}, \dots} n_s g_s \mu_B J_s \mathcal{B}_{J_s}(z_s),$$

$$z_s \equiv \frac{g_s \mu_B J_s H}{k_B T},$$

$$\mathcal{B}_J(z) = \frac{2J+1}{2J} \coth\left(\frac{2J+1}{2J}z\right) - \frac{1}{2J} \coth\left(\frac{1}{2J}z\right) \quad (1)$$

should yield the minute concentrations  $n_s$  of Fe- (and other) ions which are presumed to be evenly and individually distributed throughout the sample (no clustering). In the above formula,  $\chi_L$  is the Larmor diamagnetic susceptibility,  $J_s$  the effective spin value of species  $s$  ( $\text{Fe}^{3+}$  ( $J=5/2$ ),  $\text{Fe}^{2+}$  ( $J=2$ ), but in principle also  $\text{Cr}^{3+}$  ( $J=3/2$ ),  $\text{Ti}^{3+}$  ( $J=1/2$ ), etc.) and  $g_s$  its Landé's factor.  $\mu_B$  is Bohr's magneton,  $k_B$  Boltzmann's constant and  $\mathcal{B}_J(z)$  is the usual Brillouin function. Because of the best fit, typically Fe is believed to be present as  $\text{Fe}^{3+}$  only [27]. But there is more to this point of view.

Representative experimental data are shown in Fig. 1 for the case of a Duran glass' small shard. More details of the investigation in the Supplementary Informations (SI) for this paper. In agreement with current beliefs [27], we take  $g=2.0$  for both  $\text{Fe}^{2+}$  and  $\text{Fe}^{3+}$  paramagnetic species in the Larmor-Langevin (LL) best-fit of the data for silicates. There are cases in the literature where EPR resonances for  $g=1.9$  and  $2.1$  are found, e.g. for  $\text{Ti}^{3+}$  in high concentrations for a boro-silicate glass [28]. We stress, however, that in view of the universality tests below, using (unascertained)  $g \neq 2$  values for the Fe-ions would not change our qualitative conclusions even when different  $g_s$ -values for different paramagnetic  $s$ -species are employed.

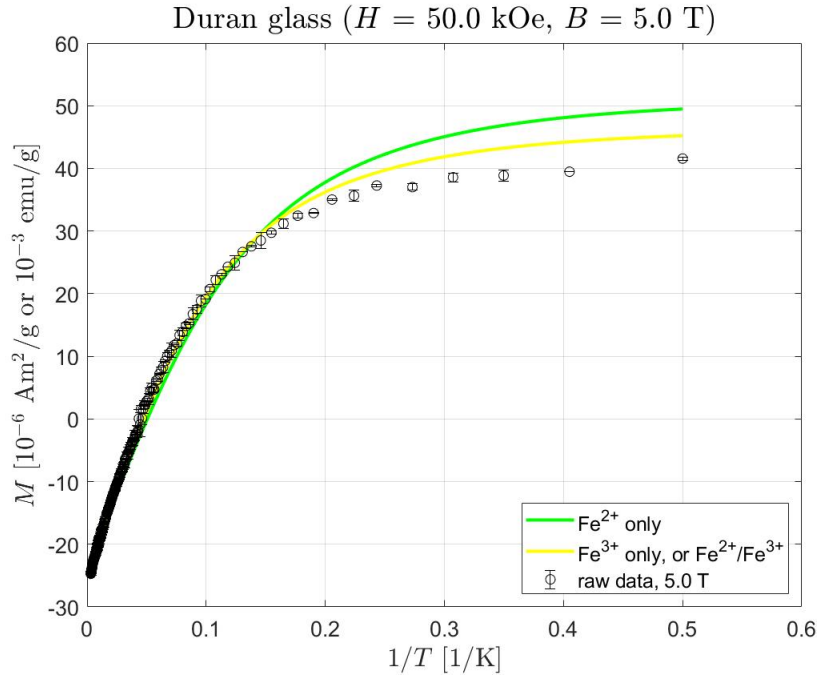


Figure 1: Duran sample's measurement of the magnetisation  $M$  at  $H=50.0$  kOe (5.0 T) in a SQUID-magnetometer. Raw data (black dots, with errorbars) being best fitted with Eq. (1) and one paramagnetic species, or two (in which case the  $\text{Fe}^{3+}$ -only scenario is always selected).

One would conclude from the above measurement and LL best-fit, Fig. 1, that the sample contains only  $\text{Fe}^{3+}$  with a concentration  $n(\text{Fe})=1.539 \times 10^{18} \text{ g}^{-1}$  [some 158 ppm] and with a Larmor susceptibility  $\chi_L=5.030 \times 10^{-7} \text{ emu/gOe}$  (or  $\text{cm}^3/\text{g}$ ). Though the above is one of our worst-case examples, the agreement between our data and expression (1) is generally unsatisfactory for all studied samples, indicating that an extra contribution is missing. We also notice that: 1) The data agreement with the LL form, Eq. (1), is generally worst at the lowest temperatures and fixed  $H$ , even for the  $\text{Fe}^{3+}$ -only scenario and will not improve by allowing other contaminants having  $J_s < 5/2$  in the best-fit. Imposing the  $\text{Fe}^{2+}$ -only scenario (thus yielding  $2.027 \times 10^{18} \text{ g}^{-1}$  [some 208 ppm] of Fe) makes the disagreement much worse; 2) This naively SQUID-extracted Fe-concentration is somewhat in disagreement with the result from our own very precise mass-spectrometry (Inductively-Coupled Plasma Mass Spectrometry, ICP-MS, hereafter referred simply as MS) analysis of the sample giving  $n(\text{Fe})=(1.469 \pm 0.006) \times 10^{18} \text{ g}^{-1}$  only [meaning  $151.0 \pm 0.6$  ppm]; moreover, a quick textbook-formula [26] estimate of Larmor susceptibility yields for Duran:  $\chi_L \simeq 4.03 \times 10^{-7} \text{ emu/gOe}$ ; 3) It is very

surprising that  $\text{Fe}^{3+}$  should be considered predominant in the Duran shard, because of the faint greenish tinge of the specimen (Figs. 1(a–c) in the SI) like in most ordinary clear silicate glass items which indicates rather  $\text{Fe}^{2+}$  predominance [29].

We have carried out a range of SQUID-runs both with  $H$ - and  $T$ -fixed, reaching the conclusion that LL-based theory fits of SQUID-data are unreliable for glasses without a fuller interpretation (more below). Moreover, as we shall demonstrate in this paper, the missing contribution that comes from the glass itself when hypothetically cleaned of all paramagnetic impurities is a new and rather fascinating phenomenon with important implications for glass science and technology.

**B. Full BK7 glass analysis.** As expected and as shown below, the case of BK7 is that of a very pure and micro-crystal free glass, so we have conducted most of our study on this system. Tables 1 and 2 as well as Fig. 7 in the SI show significant fluctuations in both  $n(\text{Fe})$  and  $\chi_L$  by SQUID-scanning in  $T$  or  $H$  while keeping  $H$  or  $T$  constant, respectively, and employing the LL-fit form, Eq. (1).

Magnetic Field (kOe)	1.0	2.5	5.0	10.0	20.0	30.0	40.0	50.0	65.0	MS
BK7 LL-parameters										
$n(\text{Fe}^{3+}) 10^{17} \text{ g}^{-1}$	1.888	1.849	1.845	1.849	1.867	1.888	1.906	1.914	1.931	$1.657 \pm 0.019$
$\chi_L 10^{-7} \text{ emu/gOe}$	3.922	4.064	4.139	4.257	4.277	4.283	4.295	4.294	4.297	-
$n(\text{Fe}^{2+}) 10^{17} \text{ g}^{-1}$	2.752	2.690	2.667	2.621	2.559	2.541	2.536	2.526	2.526	$1.657 \pm 0.019$
$\chi_L 10^{-7} \text{ emu/gOe}$	3.922	4.064	4.136	4.249	4.262	4.266	4.277	4.276	4.278	-

Table 1: LL-fitting parameters (Eq. (1)) extracted from different SQUID runs of  $M$  vs.  $1/T$  at stated  $H$ -values for a BK7-prism chip. The first row is obtained from best fits when both  $\text{Fe}^{3+}$  and  $\text{Fe}^{2+}$  species are allowed (in practice one always obtains  $n(\text{Fe}^{2+})=0$ ); for comparison, the results when  $\text{Fe}^{2+}$ -only is allowed are shown in the second row. The precise MS value of  $n_{MS}(\text{Fe})$  is also indicated (errorbar was estimated from spectrometer specifications and by dissolving several separate BK7-prism chips, including this one).

Temperature (K)	2.0	4.5	7.5	10.0	20.0	MS
BK7 LL-parameters						
$n(\text{Fe}^{3+}) 10^{17} \text{ g}^{-1}$	1.746	1.877	1.969	2.035	3.135	$1.657 \pm 0.019$
$\chi_L 10^{-7} \text{ emu/gOe}$	4.178	4.269	4.326	4.350	4.686	-
$n(\text{Fe}^{2+}) 10^{17} \text{ g}^{-1}$	2.414	2.905	3.358	3.681	6.206	$1.657 \pm 0.019$
$\chi_L 10^{-7} \text{ emu/gOe}$	4.178	4.269	4.326	4.350	4.686	-

Table 2: The same as in Table 1, but as extracted from SQUID-runs of  $M$  vs.  $H$  at stated  $T$ -values.

From the naive SQUID-characterisation one would deduce (say, at  $H=65.0$  kOe (6.5 T)) concentrations  $n(\text{Fe}^{2+})=0$  and  $n(\text{Fe}^{3+})=1.931 \times 10^{17} \text{ g}^{-1}$  [some 21 ppm] while from our precise MS analysis we find  $n_{MS}(\text{Fe})=(1.657 \pm 0.02) \times 10^{17} \text{ g}^{-1}$  [only  $17.5 \pm 0.2$  ppm]. The disagreement with the (true) MS value of  $n(\text{Fe})$  is again particularly severe when obtained by imposing  $\text{Fe}^{2+}$ -only (majority species, as it ought to be [29]), yielding  $2.526 \times 10^{17} \text{ g}^{-1}$  [some 27 ppm] of Fe at 65.0 kOe) and especially for  $M$  vs.  $H$  SQUID-runs (Table 2). But even for  $\text{Fe}^{3+}$ -only and for  $M$  vs.  $1/T$  the disagreement is remarkable and  $n(\text{Fe}^{3+})$  appears to be  $H$ -dependent (Table 1) or  $T$ -dependent (Table 2).

A way to resolve the discrepancy might be to increase the parameter space and include other (minority) paramagnetic species. Some of which are indeed present, as shown in Table 3.

Fe	Ti	V	Cr	Mn	Co	Ni	Cu
1	0.1	0	0.1	0.01	0	0.01	0.01

Table 3: Relative concentration (taking  $n(\text{Fe})=1$ ) of all other Fe-group magnetic elements present in the same BK7-chip SQUID-characterised in this work and from our own qualitative MS analysis.

However, only Ti (with a  $J_s=1/2$  if  $\text{Ti}^{3+}$  (which is doubtful in the silicates)) and  $\text{Cr}^{3+}$  ( $J_s=3/2$ ) are present in noticeable concentrations and their presence in Eq. (1) does not improve the best-fits at all, since one

obtains again that only  $\text{Fe}^{3+}$  should be present (due to its highest  $J_s$  available) and all other species with  $J_s < 5/2$  have  $n_s=0$ . An improvement would follow were other paramagnetic species with  $J_s \geq 5/2$  also present (like  $\text{Mn}^{2+}$ ,  $\text{Co}^{2+}$  ... or the rare-earth metals) but these are basically all absent.

To get to the root of the discrepancy, we have re-plotted all available SQUID-runs data as  $M - M_L$  ( $M_L = -\chi_L H$ ) vs.  $H/T$  which according to the generalised LL-expression in Eq. (1) should yield a universal curve. This, however, is not the case as seen in Figs 2(a),(b) and particularly for fixed  $T$  data.

Clearly there is a contribution to  $M(T, H)$  from the sample that is not accounted for by the LL-expression Eq. (1), regardless of how many paramagnetic species get included. The unaccounted difference  $M(T, H) - M_{LL}(T, H)$  is *intrinsic* to the glass itself and not vanishing should all paramagnetic impurities be removed from the sample. The unaccounted term,  $M_{intr}(T, H)$ , is clearly not a function of  $H/T$  alone, but has pieces that depend separately on  $T$  and  $H$ . At small  $H/T$  this contribution must account for the disagreement between SQUID's LL-assessed  $n(\text{Fe})$  values and the MS's  $n(\text{Fe})$  values (and so  $M_{intr}(T, H)$  mimicks the Langevin paramagnetic behaviour in this limit [14]), but at lower  $T$  or higher  $H$  something new must emerge. We remark that clustering of  $\text{Fe}^{3+}$  ions, e.g. in  $\text{O}=\text{Fe}-\text{O}-\text{Fe}=\text{O}$  formation, would just "segregate" some Fe in the glassy net and lead to lower, not higher, SQUID-ascertained  $n(\text{Fe})$  values.

In order to reveal what  $M_{intr}(T, H)$  may look like, we simply subtract the Langevin contribution (or full LL-contribution to improve clarity) with the MS known  $n(\text{Fe})$  concentration ( $(1.657 \pm 0.019) \times 10^{17} \text{ g}^{-1}$  in this case) and best-fit determined  $\chi_L$  susceptibility values. The relative % fractions  $x_2$  of  $\text{Fe}^{2+}$  and  $x_3$  of  $\text{Fe}^{3+}$  ( $x_2+x_3=1$ ) are difficult to ascertain at such low concentrations. EPR requires interpretation and knowledge of the precise location of the two species in the glassy net (which is lacking). Mössbauer spectroscopy also does not help at such low Fe-concentrations. Thus we resort to plotting  $M_{intr}(T, H)$ -data by subtracting variable fractions  $x = x_2$  of  $\text{Fe}^{2+}$  and  $1 - x = x_3$  of  $\text{Fe}^{3+}$  Langevin-contributions. In Fig. 3(a) we present one case of what we observe at  $H=20.0$  kOe (2.0 T) for BK7 as a function of  $x$  (more cases being presented in the SI for the other glasses). Also, in Fig. 4(a) we show the case  $T=4.5$  K as a function of  $x$  (more cases in the SI).

We observe a peculiar, exotic behaviour of the ensuing intrinsic magnetisation: both as a function of  $1/T$  and as a function of  $H$ ,  $M_{intr}$  displays a broad peak instead of saturating to a constant at low temperatures and, respectively, at high magnetic fields as ordinary spin- and also orbital-paramagnetism should do. As Figs. 3(a) and 4(a) clearly show, this unusual broad peak is always present and is independent of  $x = x_2$ , so this first conclusion comes from no theoretical input at all. To fit the data carefully – understanding the physical origin of the broad peaks, how they move by changing  $H$  and  $T$ , respectively, and explaining the Fe-concentration mismatch – a new theory approach is however required.

**C. Looking through other glasses.** As stated in the Introduction, we have also investigated samples of Duran and BAS glasses which, however, turned out to have much higher Fe-contamination. Nevertheless, our conclusions remain the same as for BK7 and receive much increased confidence.

As is shown in the SI, the same lack of universality for  $M(T, H)$  data sets as functions of  $H/T$  re-presents itself, particularly severe for Duran. Dissolving several Duran glass shards from the same item, we were able to determine, from MS,  $n_{MS}(\text{Fe})=(1.469 \pm 0.006) \times 10^{18} \text{ g}^{-1}$  [or  $151.0 \pm 0.6$  ppm] which we used to chart out some of the  $M_{intr}(T, H)$  glass-intrinsic magnetisation behaviour (Fig. 5 and in the SI). In spite of the much higher Fe-content,  $M_{intr}(T, H)$  resulted to be also much more intense and the broad peaks more pronounced than in BK7. This is exemplified in Figs 5(a) and 5(b) where, for comparison, a case for BK7 and the cases for BAS-p and BAS-w, see below, are also reported. Again, the broad peaks in the  $T$ - and  $H$ -dependences of  $M_{intr}$  are confirmed and, as shown in the SI, are also qualitatively independent of  $x$  ( $\text{Fe}^{2+}$ -fraction in  $n(\text{Fe})$ ). We have also sintered and vitrified two separate samples, in the form of small pellets, of Heraeus's IP-211-clear (a type of BAS) paste following the manufacturer's instructions. One of the samples, which we term BAS-p, presented a glassy appearance and residual pink coloration (Fig. 1(a) in the SI). The other – the sol-gel paste dried much longer and calcinated at 1000 C before vitrification – presented a perlaceous appearance and residual white coloration and we term this BAS-w. The coloration is an indication of the average size of the fused multi-silicate micro-spheres present within the sol-gel original paste (of a dark-violet colour). Hence, we retain that the BAS-p sample had a larger – and less dispersed – average-size in the final micro/mesoscopic clustering than the BAS-w sample (see theory below).

The most interesting results (Fig. 5) appear to be for the BAS samples, where the intensity of the intrinsic glass-magnetism appears to increase at the lowest  $T$  with heat treatment (in going from BAS-p to BAS-w). As for the Fe-concentration, from mass spectroscopy we were able to determine a staggering  $n_{MS}(\text{Fe})=(7.165 \pm 0.032) \times 10^{18} \text{ g}^{-1}$  [ $958.1 \pm 4.3$  ppm] from a series of calcinated BAS-paste flakes. This again contrasts with a naive SQUID-magnetisation LL-ascertained value (e.g. at  $H=50.0$  kOe)  $n(\text{Fe}^{3+})=7.295 \times 10^{18} \text{ g}^{-1}$

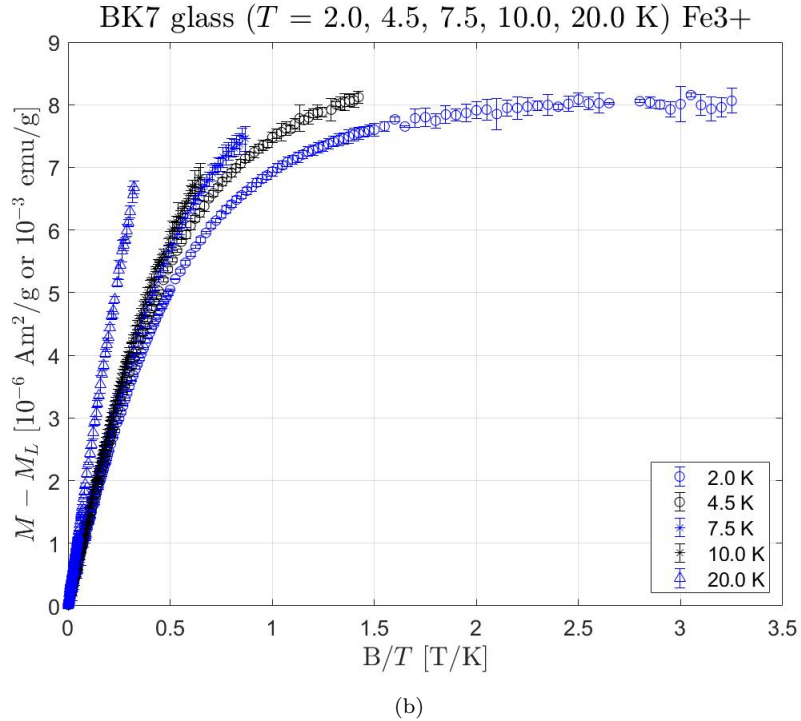
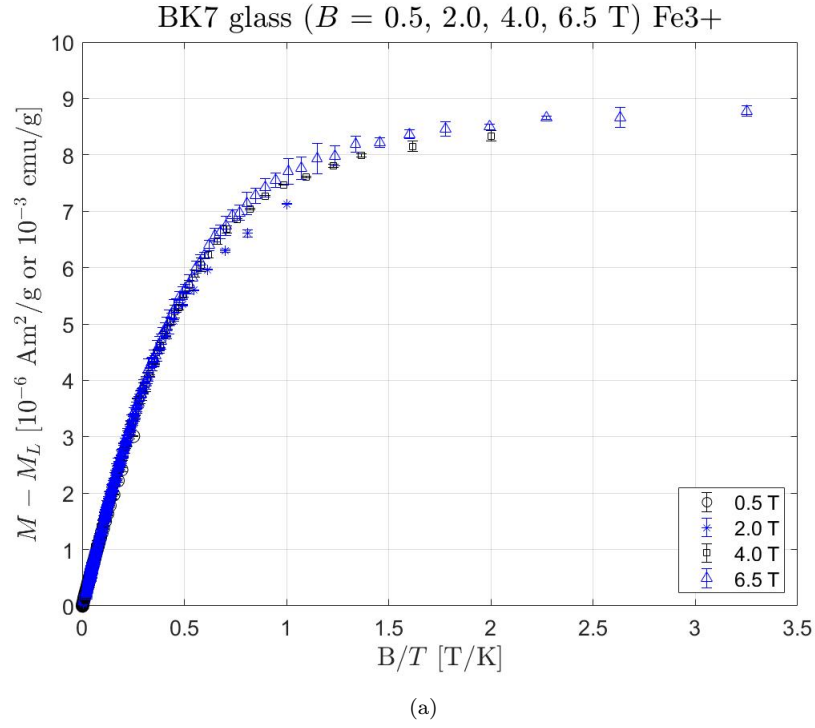


Figure 2: Universality test for our SQUID-run measurements on BK7: (a) with fixed  $H$  as stated (in Tesla) and (b) with fixed  $T$  as stated. For clarity, in panel (a) not all of our fixed- $H$  runs are reported. Fe<sup>3+</sup> means that the subtracted Larmor values refer to the best-fit of raw data with the extended LL expression, Eq. (1), which always singles out the Fe<sup>3+</sup>-only scenario. As always, here  $B = \mu_0 H$ .

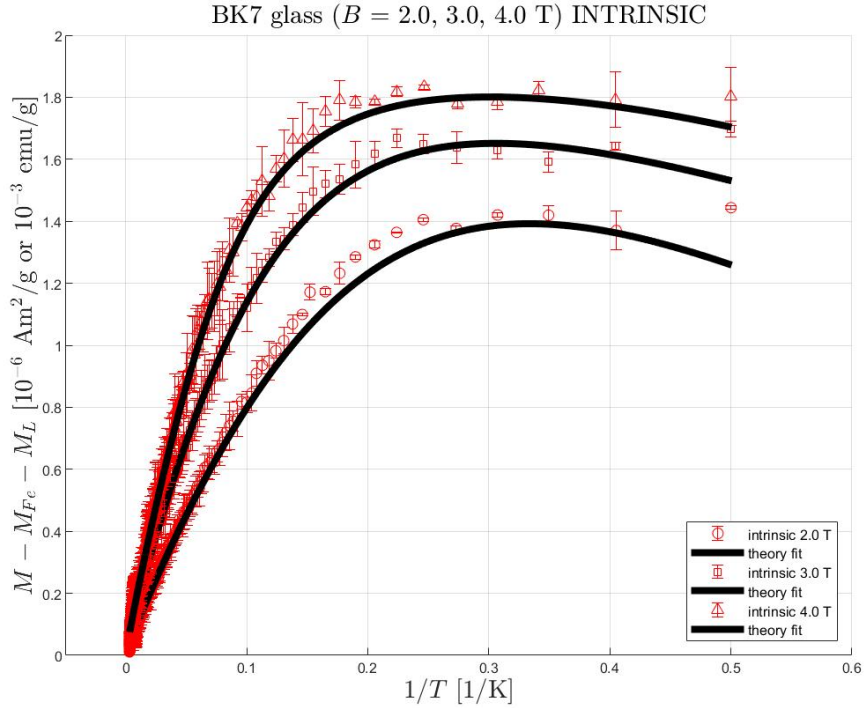
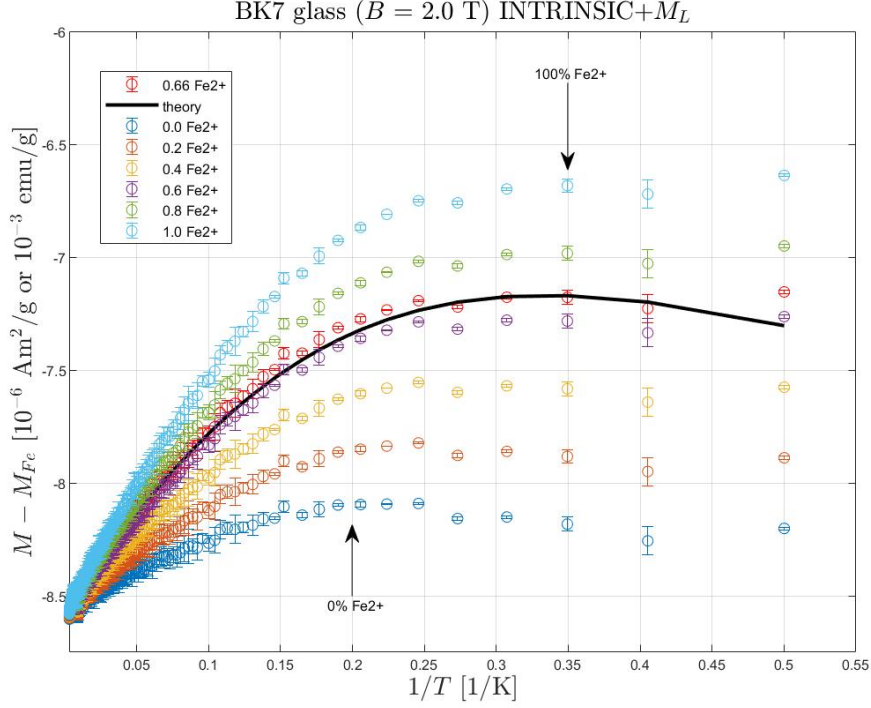


Figure 3: (a) Re-plot of raw data after subtraction of the Langevin contribution from  $x n_{MS}(\text{Fe}) \text{Fe}^{2+}$ -ions and  $(1-x) n_{MS}(\text{Fe}) \text{Fe}^{3+}$ -ions with  $n_{MS}(\text{Fe})=1.66 \times 10^{17} \text{ g}^{-1}$  (the MS value, see text); from top to bottom  $x = x_2=1.0, 0.8, 0.6, 0.4, 0.2, 0.0$ ; the value  $x=0.66$  is selected by theory (see below) and the theory fit (full curve) is also drawn. (b) At fixed value  $x = x_2=0.66$  selected by theory, the re-plotted  $M_{intr}$  data points (obtained by subtraction from raw data) shown for various  $B$ -values ( $B = \mu_0 H$ ) and compared to theory fitting curves.

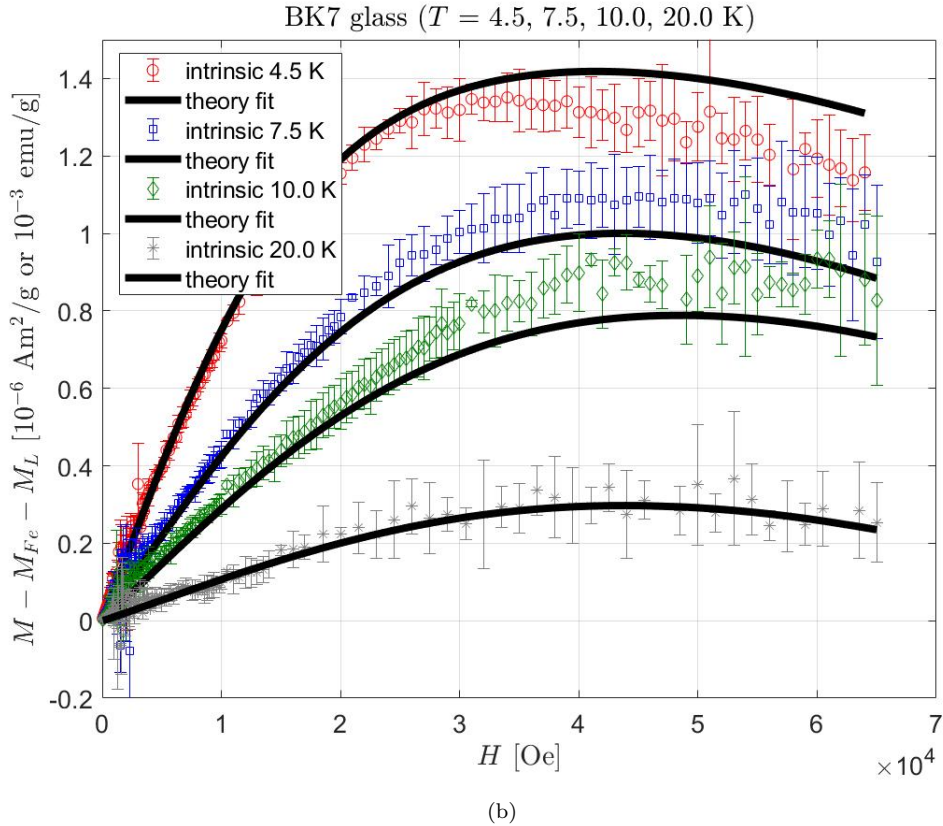
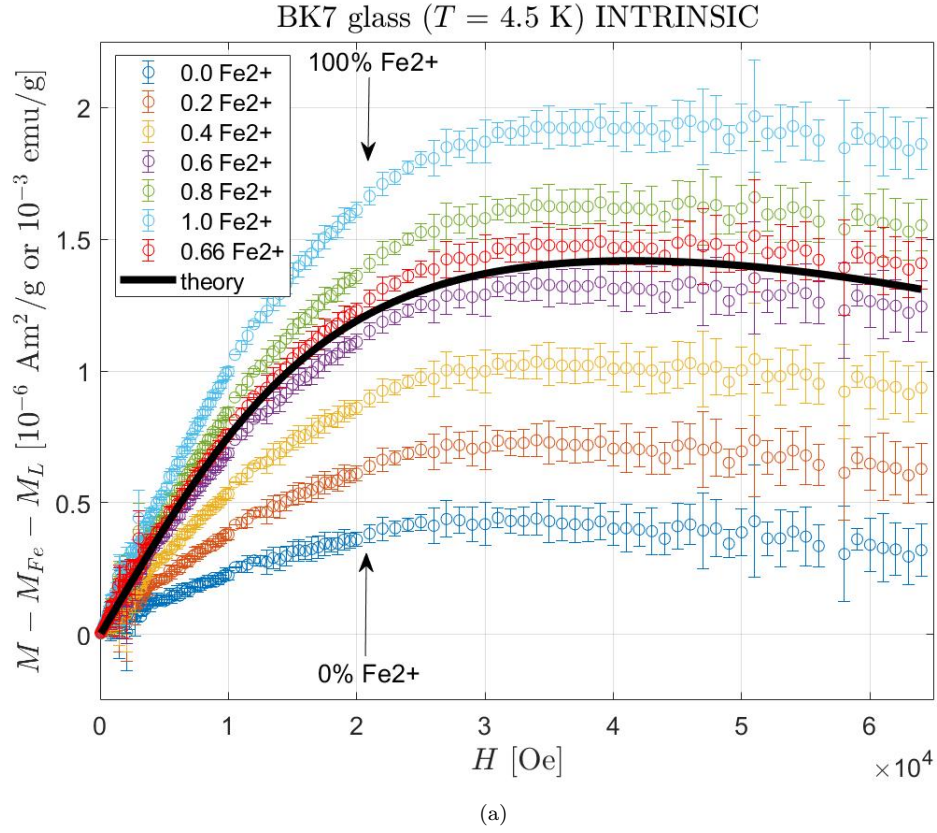


Figure 4: (a) As for Fig. 3(a), but for  $M_{intr}$  at fixed  $T=4.5$  K. (b) As for Fig. 3(b), but for various  $T$ -values and compared to theory fitting curves. On the horizontal axis  $H$  in Oe ( $\times 10^4$ ) or  $B$  in T ( $B = \mu_0 H$ , as always).



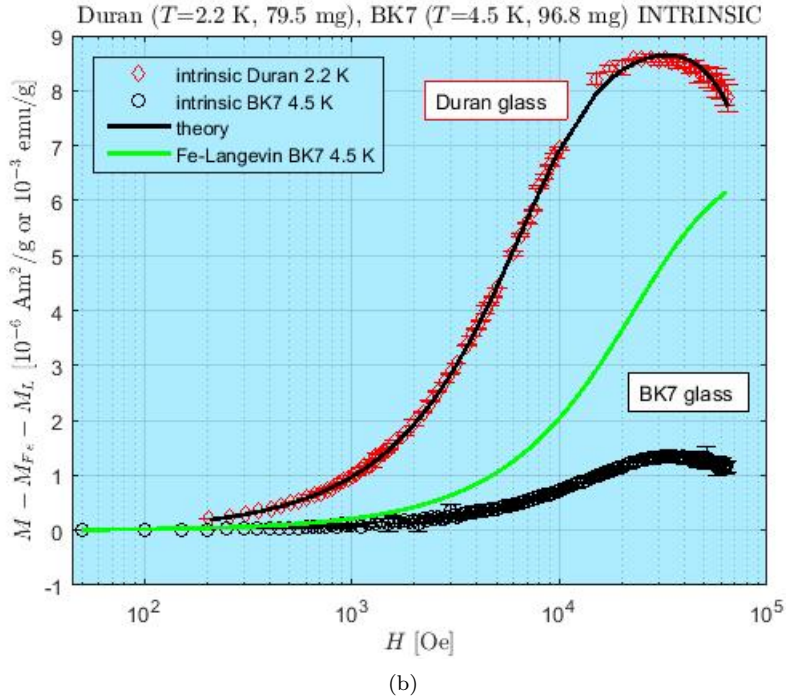
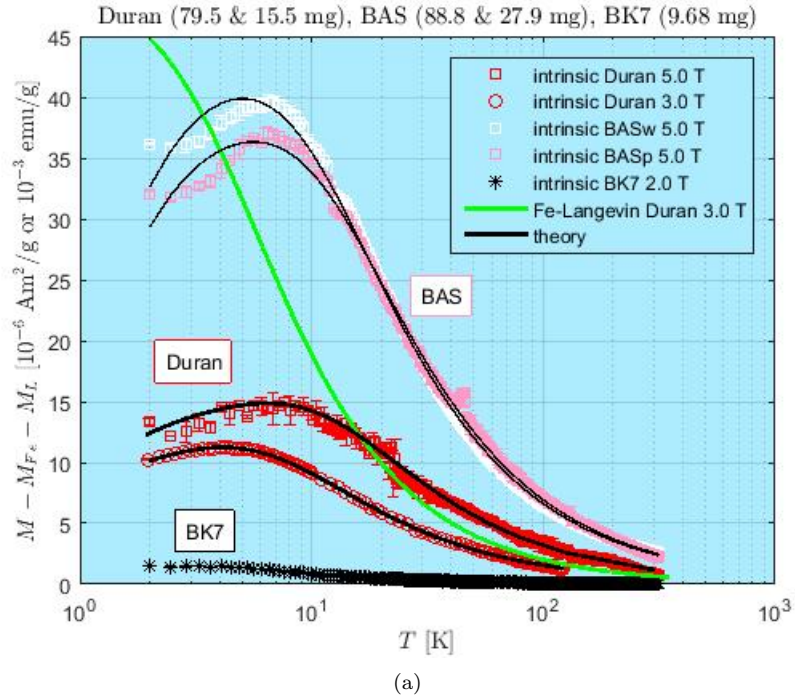


Figure 5: (a) A few “experimental” curves (with theory fits) for  $M_{intr}$  for the two other glasses, Duran and BAS, as a function of  $T$  and for the  $x = x_2$   $\text{Fe}^{2+}$ -fraction selected by the theory fit (BK7 also shown for comparison):  $x_{\text{BK7}}=0.66$ ,  $x_{\text{Duran}}=0.83$  and  $x_{\text{BAS}}=0.63$  (both -p and -w type). The green curve is the Langevin Fe-contribution for Duran at 3.0 T. (b) “Experimental” curve (with theory fit) for  $M_{intr}$  for Duran, as a function of  $H$  (BK7 also shown for comparison):  $x_{\text{BK7}}$  and  $x_{\text{Duran}}$  as in (a). More cases and theory comparison in the SI. The green line is the Fe-Langevin for BK7 at 4.5 K. Sample masses serve to identify different samples.

[some 976 ppm] (or  $n(\text{Fe}^{2+})=9.634 \times 10^{18} \text{ g}^{-1}$  [some 1288 ppm] in both cases with a bad fit at the lower temperatures).

We characterised  $M_{\text{intr}}(T, H)$  using the same subtraction procedure as for BK7. Despite the much increased Fe-contamination, for both Duran and BAS systems the intrinsic contribution remains clearly ascertained and for BAS it is the strongest for the three systems investigated. All three systems display the possible presence of oscillations in  $M_{\text{intr}}(T, H)$  vs.  $T$  at the lowest temperatures investigated ( $T < 3 \text{ K}$ , see the SI).

**D. Intrinsic magnetisation temperature oscillations.** To conclude the survey of our novel observations, we report that by re-plotting the intrinsic magnetisation  $M_{\text{intr}}(H, T)$  as a function of temperature  $T$  in a linear scale some distinct oscillations for fixed  $H$  as a function of  $T$  in the intermediate range are observed. These cannot be mistaken with spurious instrumental effects and are clearly visible above the SQUID instrumental errorbars. Moreover, they are present for all three glassy systems investigated and in different conditions. In Fig. 6 we report the clearest cases, those for borosilicate Duran at  $B=3.0 \text{ T}$  and especially at  $5.0 \text{ T}$ . As discussed in the SI, we believe the origin of these oscillations lies in the dynamics of the non-spherical solid-like cells making up the amorphous solid and in the response to the cells' dynamics of the charged tunneling (magnetic-field coupled) fluid particles in the cell-cell interspace “voids”. Interestingly, these oscillations may well be related to the “Boson peak” phenomenology [16] and have the same basic explanation.

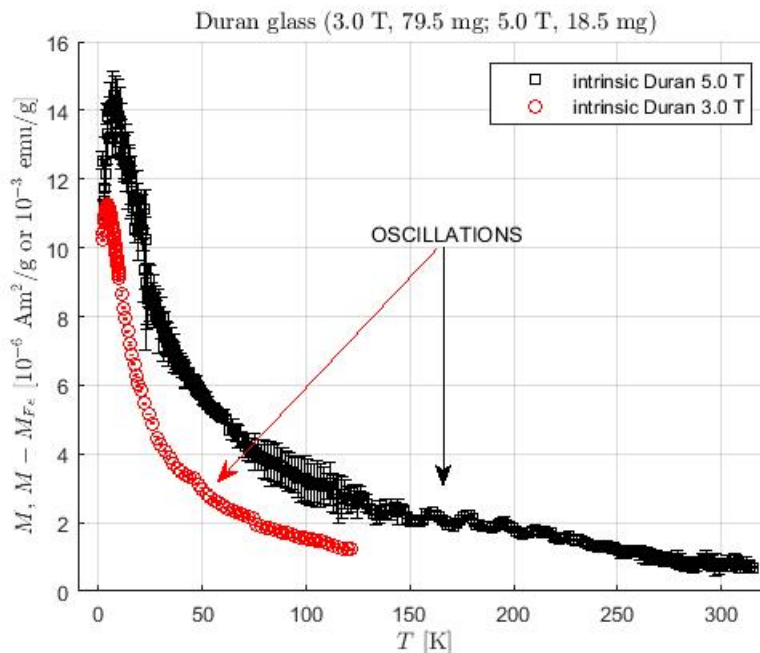


Figure 6: Duran samples’ raw-data deduced intrinsic magnetisation (after subtraction of electronic-Larmor and Fe-Langevin contributions) as a function of temperature for  $B=3.0 \text{ T}$  (red symbols) and for  $5.0 \text{ T}$  (black). Distinct oscillations in the intermediate temperature range are clearly visible, especially for the  $5.0 \text{ T}$  case, and well above the instrumental errorbar range). They are also observed for the BAS-p sample (see SI).

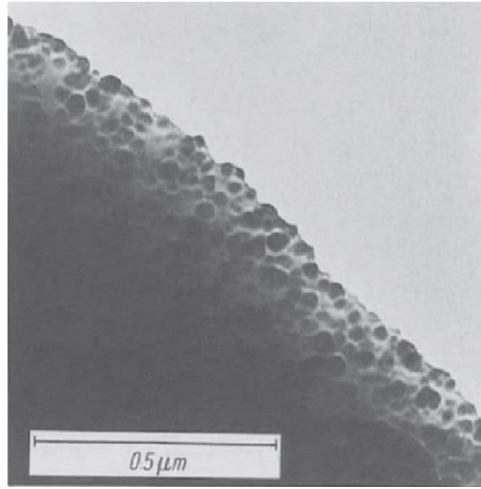
**E. Proposed theoretical explanation.** There is no standard explanation that we know of, for all these observations in the three investigated glass types. Clustering of Fe-ions is not an explanation, for  $n(\text{Fe})$  as determined from the naive LL-fitting of SQUID-data is always greater than that determined by the MS. Kramers doubling of the  $J=5/2 \text{ Fe}^{3+}$ -spin spectrum would not help, for it would result in a linear dependence of the energy levels and splittings on  $H$ . Quenching of the orbital moments for Fe-ions by the local-“crystal” field is believed to be complete in the multi-silicates anyway [27], a reason why  $g=2$  is expected to be correct here, for both  $\text{Fe}^{2+}$  and for  $\text{Fe}^{3+}$  [30].

The observed features of the intrinsic magnetisation  $M_{\text{intr}}(T, H)$  are however quantitatively consistent with the results one obtains from the theoretical scenario of intermediate-range glass structure [11, 15, 31, 32, 33] briefly outlined in the Introduction. The theory was proposed by one of us (GJ) for the explanation of the puzzling magnetic effects in dielectric (and organic) glasses [31]. There is already extensive literature on this theory, which for the magnetisation is the continuation of previous work [14] concerning the mismatch

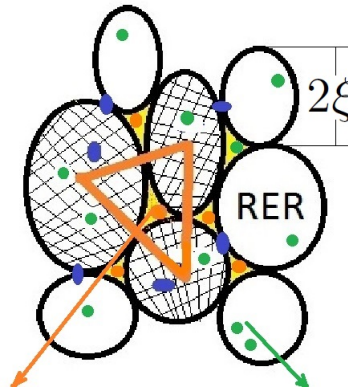
in  $n(\text{Fe})$  as deduced from published [27, 34] SQUID-data for BK7-Duran-BAS samples (not our own) and from published [34] heat-capacity data in the 300 mK - 4 K range for the Duran and BAS glasses. The present work thus sets that theory to a new test, with a much wider range of experimental data for  $M = M(T, H)$  now available. Once more, this theory carefully resolves the Fe-concentration mismatch (now between MS and naive LL SQUID-determined values). We indeed obtain, fitting our own SQUID-data with  $M = M_{LL} + M_{intr}^{tunn}$  (the latter contribution being provided by theory discussed below and in the SI): for BK7  $n(\text{Fe}) = (1.688 \pm 0.004) \times 10^{17} \text{ g}^{-1}$  [17.8  $\pm$  0.1 ppm]; for Duran  $n(\text{Fe}) = (1.471 \pm 0.006) \times 10^{18} \text{ g}^{-1}$  [151.1  $\pm$  0.6 ppm]; for BAS  $n(\text{Fe}) = (7.127 \pm 0.007) \times 10^{18} \text{ g}^{-1}$  [953.1  $\pm$  0.9 ppm]. The agreement with the data obtained from the MS analysis is thus now rather satisfactory. As is shown in the SI, the tunneling parameters are roughly the same as those obtained for the BK7-Duran-BAS 2000 samples [14], the major difference being the Fe-concentrations which are higher for our own samples. As for the strength of the tunneling intrinsic contribution, we obtain  $n_{tunn}/n_{MS}(\text{Fe})$  concentration ratios for the three systems we investigated: BK7  $(1.348 \times 10^{16} / 1.657 \times 10^{17}) = 0.081$  (8.1 %); Duran  $(4.519 \times 10^{16} / 1.469 \times 10^{18}) = 0.031$  (3.1 %); BAS  $(2.323 \times 10^{17} / 7.165 \times 10^{18}) = 0.032$  (3.2 %). This justifies our choice to concentrate our study on BK7: though the intrinsic magnetisation is the weakest, in comparison the Fe-concentration is the lowest and the ratio of intrinsic/Langevin contributions the highest for this system. Moreover, as shown in the graphs in this article, the tunneling theory explains rather well most of the new features of the intrinsic magnetisation of glasses.

Back to theory, in a nutshell the tunneling-currents approach requires to abandon the widespread view of amorphous solids as continuously- and homogeneously-disordered media at the atomic and MR scale (the CRN model, which continues to represent a useful zero-order approximation). Instead, one admits that – for a bulk glass – the DH scenario characterizing the supercooled liquid state [13] continues to be valid below  $T_g$ . Here, the “amorphous” solid state is made up of solid-like particle regions – jammed together below  $T_g$  – and liquid-like particle regions in between [11]. The solid-like regions are also known to be better-ordered as well [12, 35, 36], at least there is strong evidence just above  $T_g$  [37, 38], hence they are called RER (regions of enhanced regularity) in the glass. The particles that are more mobile – also those proximal to RER walls, which are most likely charged  $\text{O}^-$  dangling bonds for the multi-silicate glasses – get to be squeezed together in the “voids” between the solid-like RER which themselves make up a close-packed true random solid. These charged, mobile particles in the “voids” will be highly correlated and subjected to complicated forces from their surroundings. A reasonable hypothesis [31, 39] is that they will tunnel coherently as effective quasi-particles in each highly-correlated void-contained “liquid drop”, the effective “particles” having large negative effective charge  $Q$ ,  $|Q| \gg |e|$  ( $e$  is the electron’s charge) and heavily renormalized tunneling parameters [31, 39]. Each tetrahedral void between mostly four RER being composed of four faces, the quasi-particles – one for each face – will be subjected to an effective local potential having three-fold topology (or symmetry, for perfect RER local tetrahedral arrangement, then becoming a distorted three-welled tunneling potential with topological disorder in the shape, size and final location of the four RER). These quasi-particles are the sources of orbital magnetic moments (having a collective local nature) and are believed [14] to be the sources of the observed intrinsic “glass-magnetisation”  $M_{intr}^{tunn}$ . More about this model of glasses in the SI and in [11, 15].

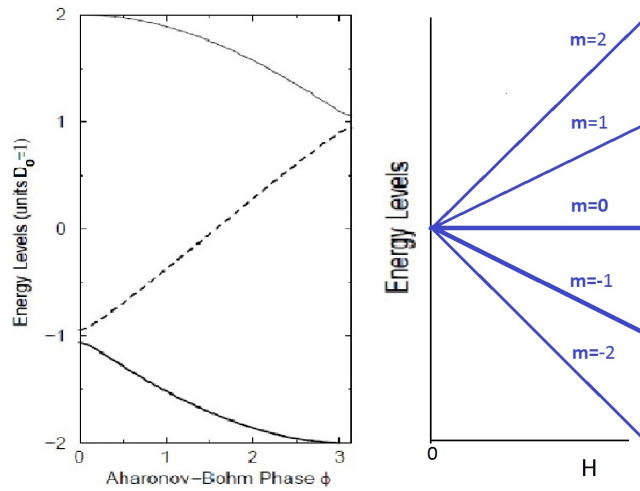
In Fig. 7(a) we show a HRTEM (high-resolution transmission electron- microscopy) image [40] of the structure of a typical silicate glass, where the random closed-packed arrangement of these RER is apparent. Vogel [41] has produced many of such HRTEM pictures for network glasses, showing that the structure here advocated for is generic for any glass [15, 11, 12]. There is in fact reasonably good agreement between the size  $2\xi$  of the RER as estimated in HRTEM and what is deduced from the concentration of the coherent-tunneling quasiparticles obtained by theory-fitting a wide spectrum of experiments on glasses in magnetic fields at Kelvin and sub-Kelvin temperatures [11]. One gets, for BK7:  $2\xi \simeq 60 \text{ nm}$ , Duran:  $2\xi \simeq 31 \text{ nm}$ , BAS:  $2\xi \simeq 32.5 \text{ nm}$ . Fig. 7(b) is a 2D-sketch of the proposed structure of glasses at the nanoscale level, with the RER containing mobile semimetal- and metal-oxide ions in their “voids” and  $\text{O}^-$  dangling bonds coating their tetrahedral voids’ faces. Their quasi-particles will be subjected to an effective three-welled tunneling potential [11, 31]. Finally, Fig. 7(c) [left panel] shows the ensuing three-level system’s [42] quanto-mechanical energy levels for a quasi-particle in the three-welled effective model [31] describing the collective coherent-tunneling of all the  $N_{tunn}$  charged  $\text{O}^-$  particles sitting on a face of the distorted-tetrahedral void geometry. Clearly, this is a non-linear energy spectrum in  $H$  and the idea is that this spectrum is in part responsible for deviations from universality in  $H/T$  in the  $M - M_L$  reduced magnetisation, Figs 2(a),(b). In fact, as it turns out, the broad peak in the  $M_{int}(T, H)$  vs.  $H$  data (Figs 4(b) and 5(b)) is but a map of this three-



(a)



(b)



(c)

Figure 7: (a) HRTEM image of a thin slice of  $\text{Li}_2\text{O-SiO}_2$  glass (28.6 %  $\text{Li}_2\text{O}$  molar fraction) [40]; the  $\text{LiO}_2$ -rich “grains” or “cells” (our own model’s RER) are clearly visible, though not the “fluid” matter that comes in between. (b) Schematic 2D representation of the structure seen in (a), with the addition of: Fe-impurities (green); double-well tunneling defects (single-particle, blue); ATS (anomalous tunneling systems, collective, orange). The criss-cross pattern denotes atomic quasi-ordering. The orange quasiparticles (on each face of a tetrahedron, in fact) experience a local tunneling potential having triangular topology.  $2\xi$  is the typical cell size (some tens of nm). Arrows point to different energy-level spectra below. (c) Left panel: Energy level spectrum of a single ATS (see [31] and SI) as a function of the Aharonov-Bohm phase  $\phi \propto H$ . Right panel: A typical energy level spectrum for a paramagnetic ion ( $J_s=2$ ).

level system's spectrum as a function of  $\phi \propto H$  ( $\phi \equiv 2\pi\mathbf{B} \cdot \mathbf{S}_\Delta/\Phi_0$ , where  $\Phi_0 = h/|Q|$  is the appropriate flux-quantum,  $S_\Delta$  the surface of the flux-threaded triangular tunneling region and  $h$  Planck's constant, see the SI and [11];  $\mathbf{B} = \mu_0\mathbf{H}$  as always). The lower energy gap of each three-level system on a tetrahedral face opens non-linearly as the magnetic field increases, hence the peculiar paramagnetic contribution at the intermediate fields. This theory has been employed to calculate the  $M_{intr}^{tunn}(T, H)$  missing contribution to be added to  $M_{LL}$  (Eq. (1)) (some details in the SI, see also [11, 14, 15]) and then fitted to our own present experimental raw data obtaining excellent fits (see SI).

The remaining phenomenon that can be accounted for is the fact that the number  $N_{tunn}$  of coherent-tunneling charged ions on each tetrahedral face appears to diminish with  $T$  at the lowest temperatures as was observed in fitting available very low- $T$  data for glasses in a magnetic field [11, 15, 33]. This can be interpreted in terms of the slow growth of the RER size  $2\xi$  with decreasing  $T$  at low temperatures, but especially in terms of the broadening (consolidation) of the RER shape which results in the narrowing of the voids in-between the RER. The process can be modelled phenomenologically as Arrhenius-activated and an exponential  $\exp\{E_0/k_B T\}$  is then involved (see SI). The fact that typical values of  $E_0$  from the best-fit of typical SQUID-run data vs.  $T$  are never larger than 0.5 K (0.043 meV) is an indication that adsorption of positively-charged metal- and semimetal-oxide ions from the RER-voids-contained "melt" onto the tetrahedral walls is enhanced by the presence of a dense covering of existing  $O^-$  dangling bonds. Typical activation energy values for  $Si^{4+}$ ,  $B^{3+}$ ,  $Al^{3+}$ ,  $K^+$ ,  $Na^+$  etc. adsorbing to a clean  $SiO_2$  wall are in fact in the meV to fraction of eV range [43]. The covering of an RER-void interface by a  $O^-$  dangling-bond layer gives rise to a highly-correlated system of tunneling charged particles in a magnetic field. As the RER-size grows at the expense of the residual melt in each void, the area becoming available to  $O^-$  species diminishes and  $N_{tunn}$  drops exponentially with decreasing temperatures (zipping-up of the RER-RER interface, see SI). We believe it is this process – crucial to the onset of the cryogenic (sub-Kelvin) properties of glasses – that is responsible for the ubiquitous broad peak of the  $M_{intr}$  as a function of  $1/T$  at the lowest temperatures. The position of this peak depends almost only on  $E_0$  and for this reason the peak basically does not shift with changing  $H$ , contrary to the peak in  $M_{intr}(T, H)$  vs.  $H$  at fixed  $T$ , which moves to higher values of  $H$  as  $T$  decreases. As is indeed observed: the agreement between theory and experiments is very satisfactory. Finally, the new – unexpected – observation in our SQUID-measurements is that there are possible further oscillations in  $M_{intr}$  at the lowest temperatures investigated (see Figs. 3(a),(b) and 5(a)) beside those already mentioned at intermediate temperatures (see Fig. 6). A hint of why these come about can be found in the SI (crossover from 2D to 3D correlated/coherent tunneling regions).

Regarding the interpretation of the data, we remark that it might be argued that at high  $H/T$  the data might be consistent with a constant value of  $M_{intr}$ . However: 1) We know of no mechanism producing a constant  $M_0$  for  $H$  above a finite threshold ( $H_0$ ) and/or for  $1/T$  above a  $1/T_0$ ; 2) The offered theoretical interpretation gives good fits with  $M_{intr}$  data presenting a broad peak for high  $H/T$  and then slowly decreasing (see the SI), but there might be further oscillations due to new collective phenomena.

**F. Conclusions.** We have reported that an exotic new form of (para-)magnetism can be revealed in the measurement of the SQUID-magnetisation in glasses and is solely due to the nanoscale structure of the vitreous state itself. Though very small (for comparison: Fe (218 emu/g), Ni (55 emu/g) at 300 K (spontaneous bulk magnetisation)) due to low concentrations and the fact that the coherent tunneling currents' magnetic moments tend to cancel each other out in each tetrahedral void, the  $M_{intr}(T, H)$  intrinsic magnetisation is very interesting in its unusual  $T$ - and  $H$ -dependence and represents a new way to look – experimentally – at glass structure and other physical properties of glasses (of all types, in fact). An important consequence of our findings when interpreted through a nanoscopic-scale cellular theory for the vitreous state's organisation is the existence of a novel type of tunneling states that residing in the voids between compact nanoscopic solid-like regions appear to survive till room temperature because of the *protection* provided by the surrounding RER. We have proposed a new research tool for the study of the physics of glasses. Studying the weak but intrinsic glass magnetism in different glass types should be a very interesting new way to look at the glass "transition" and of modelling the physical properties of all glasses in an effective and efficient new way. The *protected* new tunneling systems [31], the existence of which [42] is confirmed by this work, promise to be very interesting for applications to quantum information technology due to their own inner natural coherence.

**Materials and methods.** Extreme care was taken not to accidentally contaminate the samples, which were first SQUID- and then MS-analysed (BK7 only). A BK7 prism of ca. 3 cm length and 5 mm through size was purchased from Edmund Optics, Inc., Barrington NJ (USA) and chips were obtained by means of

a ceramic knife and rubber hammer blows. Duran samples were obtained by shattering (with the rubber hammer) a brand new Schott chemistry beaker and selecting appropriate shards for measurement. The two BAS samples were obtained by firing the Heraeus IP-211-clear sol-gel paste in small Pt-foil vessels and then carefully peeling off the foil after obtaining perlaceous, glassy consistency.

The dc magnetisation  $M$  of the studied glasses was measured by means of a Quantum Design MPMS-XL7 magnetometer based on a SQUID (Superconducting QUantum Interference Device). Cotton thread was used to suspend each sample in the center of a plastic cannula which was then inserted in the magnetometer. It was always ensured that the linear dimensions of the samples along the cannula's axis were below  $\sim 5$  mm in order to guarantee a reliable instrumental estimate of the magnetisation value from the voltage measured along the detection coils. Although the studied samples had different shapes, the weak measured absolute values of  $M$  make it safe to neglect the effects of geometric demagnetisation. The plastics of the cannula is also a type of (polymeric) glass, however the amount of material involved (thin wall) is reputed to be small in comparison to the samples'. The large size of the polymer's RER, thus the tiny concentration of the polymer glass' intrinsic magnetic moments, is also thought to ensure a negligible contribution.

The investigated ranges for temperature and magnetic field were  $2 \text{ K} \leq T \leq 320 \text{ K}$  and  $0 \text{ kOe} \leq H \leq 65 \text{ kOe}$ , respectively. The temperature scans were performed at constant magnetic field always while warming the sample after a field-cooling procedure from room temperature. Especially at low temperatures ( $T \leq 60 \text{ K}$ ), where the temperature dependence of  $M_{intr}$  is more pronounced, slow warming rates  $\sim 0.3 \text{ K/min}$  were used in order to reduce the possible effect of systematic errors in the temperature reading. The magnetic field scans were performed at constant temperature after a zero-field-cooling procedure.

ICP-MS (simply MS, in this paper) determinations were performed with a Thermo-Fisher ICAP-Q spectrometer. For BK7 and Duran weighted splinters of glass (less than 100 mg) were dissolved with ultra-pure acids (1.5 ml of HF + 0.5 ml of HCl) over a hot plate in mild boiling conditions for 90 mins. For each sample residual HF is moved away with two subsequent additions of  $\text{HNO}_3$  (1 ml each) under boiling conditions. Samples are then MS-analyzed after proper dilution.

Heraeus-IP-211-clear glass (BAS) was dissolved in harder conditions. Typically, a (ca.) 30mg specimen is treated with 1ml of HF plus 0.6 ml of HCL plus 0.2 ml of  $\text{HNO}_3$  in a sealed vessel of a Milestone Ethos One microwave oven. 450 min at  $180^\circ\text{C}$  were necessary to reach complete dissolution, due to the great difficulty in dissolving aluminosilicate clusters. Even in this case residual HF is moved away with two subsequent additions of  $\text{HNO}_3$  (1 ml each) under boiling conditions.

**Acknowledgements.** GJ acknowledges support by INFN-Pavia through Iniziativa Specifica GEO-SYM, also useful conversations with K. Bevan about silicate chemistry and with R. Santoro for hints on data-fitting. The Authors are very grateful to Giacomo Prando and Pietro Carretta of the Università di Pavia, Italy, for many discussions on this project, for carrying out the SQUID-magnetisation measurements for us and for generously providing the raw data to the PI.

**Author Contributions.** The Principal Investigator (GJ) conceived the project, chose the systems to be investigated, carried out the SQUID-data analysis and wrote the manuscript. SR made the BAS-glass samples and carried out the ICP-MS analyses of all the samples.

**Data availability.** The data that support the plots and tables within this paper and other findings of this study are available from the corresponding author upon reasonable request.

**Additional information.** Supplementary Information (SI) is available for this paper.

**Conflicting interests.** The Authors declare no competing financial interests.

## References

[\*] email: giancarlo.jug@uninsubria.it (corresponding author)

- [1] A.A. Lebedev: O Polimorfizme i Otzhige Stekla, *Trud'i Gos. Opt. Inst.* **2** 1-20 (1921) (in Russian); *ibid.*, *Izv. Akad. Nauk SSSR, Otd. Mat. Estestv. Nauk, Ser. Fiz.* **3**, 381 (1937).
- [2] J.T. Randall, H.P. Rooksby and B.S. Cooper: The Diffraction of X-Rays by Vitreous Solids and its Bearing on their Constitution, *Nature* **125**, 438 (1930); *ibid.*: X-Ray Diffraction and the Structure of Vitreous Solids – I, *Z. Kristallogr.* **75**, 196–214 (1930).
- [3] W.H. Zachariasen: The Atomic Arrangement in Glass, *J. Am. Chem. Soc.* **54**, 3841–3851 (1932); *ibid.*: The Vitreous State, *J. Chem. Phys.* **3**, 162–163 (1935).
- [4] B.E. Warren: The Diffraction of X-Rays in Glass, *Phys. Rev.* **45**, 657–661 (1934).
- [5] G. Hägg: The Vitreous State, *J. Chem. Phys.* **3**, 284–49 (1935).
- [6] E.A. Porai-Koshits: Genesis of Concepts on Structure of Inorganic Glasses, *J. Non-cryst. Sol.* **123**, 1–13 (1990).
- [7] P.H. Gaskell: The Structure of Simple Glasses: Randomness or Pattern – The Debate Goes On, *Glass Phys. and Chem.* **24**, 180–188 (1998).
- [8] A.S. Bakai: The Polycluster Concept of Amorphous Solids, Beck/Günterodt (Eds.), *Metallic Glasses I*, Topics in Applied Physics **72** (Springer-Verlag, Berlin Heidelberg 1994), p. 209–255
- [9] A.S. Bakai: *Poliklastern'ie Amorfn'ie Tela*, (Khar'kov “Synteks”, Khar'kov (Ukraine) 2013) (in Russian).
- [10] A.C. Wright: Crystalline-like Ordering in Melt-quenched Network Glasses? *J. Non-cryst. Solids*, **401** 4–26 (2014); *ibid.*: The Great Crystallite versus Random Network Controversy: A Personal Perspective, *Int. J. Appl. Glass Sci.* **5**, 31–56 (2014).
- [11] G. Jug: The Polycluster Theory for the Structure of Glasses: Evidence from Low Temperature Physics, in: *Modern Problems in Molecular Physics: Selected Reviews*, L. A. Bulavin and A. V. Chalyi (eds.) (Springer International Publishing AG (2018)), Ch. 13.
- [12] G. Jug, A. Loidl and H. Tanaka: On the Structural Heterogeneity of Supercooled Liquids and Glasses, *Euro. Phys. Lett.* **133**, 56002 (2021).
- [13] M.D. Ediger: Spatially Heterogeneous Dynamics in Supercooled Liquids, *Annu. Rev. Phys. Chem.* **51**, 99–128 (2000).
- [14] S. Bonfanti and G. Jug: On the Paramagnetic Impurity Concentration of Silicate Glasses from Low-Temperature Physics, *J. Low Temp. Phys.* **180**, 214–237 (2015).
- [15] G. Jug, S. Bonfanti and W. Kob: Realistic Tunneling Systems for the Magnetic Effects in non-metallic Real Glasses, *Phil. Mag.* **96**, 648–703 (2016).
- [16] R.B. Stephens and Xiao Liu: *Low-Energy Excitations in Disordered Solids*, (World Scientific, Singapore 2021).
- [17] W.A. Phillips (Ed.): *Amorphous Solids: Low Temperature Properties*, (Springer Verlag, Berlin 1981).
- [18] P. Esquinazi (Ed.): *Tunneling Systems in Amorphous and Crystalline Solids* (Springer Verlag, Berlin 1998).
- [19] G. Jug: The Making of a Theory of the Vitreous Solid State: “From 1 mK to 1 kK”, in: *2019 Sustainable Industrial Processing Summit and Exhibition, Vol. 1: Angell Intl. Symp. - Molten Salt, Ionic & Glass-forming Liquids*, Edited by F. Kongoli et. al. (FLOGEN Stars Outreach 2019).
- [20] J. Zmuidzinas: Superconducting Microresonators: Physics and Applications, *Annu. Rev. Condens. Matter Phys.* **3**, 169 (2012).

- [21] L. Faoro and L.B. Ioffe: Interacting tunneling model for two-level systems in amorphous materials and its predictions for their dephasing and noise in superconducting microresonators, *Phys.Rev. B* **91**, 014201 (2015).
- [22] P.V. Klimov *et al.*: Fluctuations of Energy-Relaxation Times in Superconducting Qubits, *Phys. Rev. Lett.* **121**, 090502 (2018).
- [23] R.M. Macfarlane, Y. Sun, P.B. Sellin, and R.L. Cone: Optical Decoherence in Er<sup>3+</sup>-Doped Silicate Fiber: Evidence for Coupled Spin-Elastic Tunneling Systems, *Phys. Rev. Lett.* **96**, 033602 (2006).
- [24] E. Saglamyurek *et al.*: Quantum storage of entangled telecom-wavelength photons in an erbium-doped optical fibre, *Nature Photonics* **9**, 83–87 (2015).
- [25] M. Rančić, M.P. Hedges, R.L. Ahlefeldt and M.J. Sellars: Coherence time of over a second in a telecom-compatible quantum memory storage material, *Nature Physics* **14**, 50–54 (2018).
- [26] N.W. Ashcroft and N.D. Mermin: *Solid-State Physics*, (Saunders College International, Philadelphia 1976), p. 655.
- [27] T. Herrmannsdörfer and R. König: Magnetic impurities in glass and silver powder at milli- and microkelvin temperatures, *J. Low Temp. Phys.* **118**(1–2), 45–57 (2000).
- [28] S. Davé and R.K. Maccrone: Magnetic Properties of Sol-Gel Glasses Containing Titanium Ions, *J. of Non-Cryst. Solids* **71**, 303-310 (1985).
- [29] A.K. Varshneya: *Fundamentals of Inorganic Glasses* (Academic Press Inc., Boston 1994), p. 470.
- [30] C. Kittel: *Introduction to Solid-State Physics* (8th Edition, John Wiley & Sons, New York 2005), Ch. 11.
- [31] G. Jug: Theory of the Thermal Magnetocapacitance of Multi-component Silicate Glasses at Low Temperature, *Phil. Mag.* **84**(33), 3599–3615 (2004).
- [32] G. Jug: Multiple-well Tunneling Model for the Magnetic-field Effect in Ultracold Glasses, *Phys. Rev. B* **79**, 180201 (2009).
- [33] G. Jug, M. Paliienko and S. Bonfanti: The Glassy State — Magnetically Viewed from the Frozen End, *J. Non-Cryst. Solids* **401**, 66–72 (2014).
- [34] L. Siebert: Ph.D. Thesis Heidelberg University (2001), [www.ub.uni-heidelberg.de/archiv/1601](http://www.ub.uni-heidelberg.de/archiv/1601)
- [35] T. Kawasaki, T. Araki and H. Tanaka: Correlation between Dynamic Heterogeneity and Medium-Range Order in Two-Dimensional Glass-Forming Liquids, *Phys. Rev. Lett.* **99**, 215701 (2007).
- [36] T. Kawasaki and H. Tanaka: Structural origin of dynamic heterogeneity in three-dimensional colloidal glass formers and its link to crystal nucleation, *J. Phys.: Condens. Matter* **22**, 232102 (2010).
- [37] H. Tong and H. Tanaka: Revealing Hidden Structural Order Controlling Both Fast and Slow Glassy Dynamics in Supercooled Liquids, *Phys. Rev. X* **8**, 011041 (2018).
- [38] H. Tanaka, H. Tong, R. Shi and J. Russo: Revealing key Structural Features hidden in Liquids and Glasses, *Nature Reviews Phys.* **1**, 333–348 (2019).
- [39] G. Jug and M. Paliienko: Multilevel Tunneling Systems and Fractal Clusters in the Low-Temperature Mixed Alkali-Silicate Glasses, *Sci. World J.* **2013**, 1–20 (2013).
- [40] W. Vogel, L. Horn, H. Reiss and G. Volksch: Electron-Microscopical Studies of Glass, *J. Non-Cryst. Solids* **49**, 221-240 (1982); see also W. Vogel: *Glass Chemistry* (2nd edn., Springer, Berlin 1992), p. 74
- [41] W. Vogel: *Struktur und Kristallisation der Gläser* (VEB Deutscher Verlag für Grundstoffindustrie, Leipzig 1965).



- [42] Three-level systems are a reality in glasses: A.-M. Boiron, Ph. Tamarat, B. Lounis, R. Brown, and M. Orrit: Are the spectral trails of single molecules consistent with the standard two-level system model of glasses at low temperatures? *Chem. Phys.* **247**, 119–132 (1999).
- [43] R. Memming: *Semiconductor Electrochemistry* (Wiley-VCH Verlag, Weinheim (Germany) 2001), Chs. 5-6